

# UC Irvine

## UC Irvine Previously Published Works

### Title

Network Connectivity of the Right STS in Three Social Perception Localizers

### Permalink

<https://escholarship.org/uc/item/2zx7022k>

### Journal

Journal of Cognitive Neuroscience, 29(2)

### ISSN

0898-929X

### Authors

Dasgupta, Samhita

Tyler, Sarah C

Wicks, Jonathan

et al.

### Publication Date

2017-02-01

### DOI

10.1162/jocn\_a\_01054

### Copyright Information

This work is made available under the terms of a Creative Commons Attribution License, available at <https://creativecommons.org/licenses/by/4.0/>

Peer reviewed

# Network Connectivity of the Right STS in Three Social Perception Localizers

Samhita Dasgupta<sup>1</sup>, Sarah C. Tyler<sup>2</sup>, Jonathan Wicks<sup>1</sup>,  
Ramesh Srinivasan<sup>1</sup>, and Emily D. Grossman<sup>1</sup>

## Abstract

■ The posterior STS (pSTS) is an important brain region for perceptual analysis of social cognitive cues. This study seeks to characterize the pattern of network connectivity emerging from the pSTS in three core social perception localizers: biological motion perception, gaze recognition, and the interpretation of moving geometric shapes as animate. We identified brain regions associated with all three of these localizers and computed the functional connectivity pattern between them and the pSTS using a partial correlations metric that characterizes network

connectivity. We find a core pattern of cortical connectivity that supports the hypothesis that the pSTS serves as a hub of the social brain network. The right pSTS was the most highly connected of the brain regions measured, with many long-range connections to pFC. Unlike other highly connected regions, connectivity to the pSTS was distinctly lateralized. We conclude that the functional importance of right pSTS is revealed when considering its role in the large-scale network of brain regions involved in various aspects of social cognition. ■

## INTRODUCTION

As social beings, humans navigate complex interactive encounters on a daily basis, an ability that requires correctly interpreting facial and body cues that signal the goals and intentions of others. In the past 20 years, noninvasive brain imaging methods together with neurophysiological studies have identified key cortical regions in the so-called “social brain” (coined by Brothers, 1990), which is involved in processing and interpreting the actions and intentions of other individuals. This network consists of several regions, including the posterior extent of the STS (pSTS), fusiform gyrus, the inferior frontal gyrus (IFG), and the anterior insula. Each of these brain regions is believed to contribute a unique function to the larger network, with the more posterior of these brain sites (pSTS and fusiform) associated with visual perception of social cues, the IFG associated with the interpretation and planning of actions, and pFC linked to the attribution of mental states to external objects and events (Menon & Uddin, 2010; Krueger, Barbey, & Grafman, 2009; Miller & Cohen, 2001).

In this study, we focus on the STS, the posterior extent (pSTS) of which has been implicated as a critical module for perception of actions, faces, eye gaze, and animacy (Carter & Huettel, 2013; Shultz & McCarthy, 2012; Caspers, Zilles, Laird, & Eickhoff, 2010; Carrington

& Bailey, 2009; Van Overwalle, 2009; Hein & Knight, 2008; Gobbini, Koralek, Bryan, Montgomery, & Haxby, 2007). This study seeks to characterize the pattern of network connectivity emerging from the pSTS when engaged in social perception tasks. This approach is motivated by the notion that functional specialization is not just reflected in the local activity within a single brain site but also in the coordination of information flow throughout the network. Although the literature has been quite successful at mapping brain regions involved in social cognition, very few have attempted to characterize the actual information pathways through this large-scale brain system. We also note that the pSTS and social perception, more broadly, are not well characterized by a localizationist approach. The strongest model of social cognitive dysfunction is autism, which is associated with atypical patterns of long-range functional connectivity as compared with neurotypicals in the social cognition brain network (specifically hypoconnectivity, as assessed in the resting state; von dem Hagen, Stoyanova, Rowe, Baron-Cohen, & Calder, 2013; Anderson et al., 2011). From this, we conclude that a critical feature for understanding the brain-behavior relationship for social perception may be found in the pattern of long-range connectivity.

The goals of this study are to test the hypotheses that the pSTS is a major hub for the large-scale cortical network of the “social brain” and to identify those patterns of connectivity through the pSTS that are specialized for the analysis of distinct social cognitive cues. To understand the large-scale network, we compute the

---

<sup>1</sup>University of California, Irvine, <sup>2</sup>University of California, San Diego

functional connectivity pattern between the pSTS and related brain regions using partial correlations. This approach has some major advantages over pairwise Pearson correlation (also termed “full correlation”) as a means for assessing functional connectivity. The full correlation reflects the linear dependence between brain regions, a relationship that labels both direct and indirect connections indiscriminately, including common driving inputs and other shared influences that may be epiphenomenal to the task of interest. Functional connectivity computed from full correlations are particularly susceptible to artificial inflation from physiological artifacts such as subject motion (Power, Barnes, Snyder, Schlaggar, & Petersen, 2012). Some of the limitations inherent to full correlations can be overcome by examining covariation structure computed from partial correlations, which identifies variance unique to any pair of regions and not shared with the other brain regions included in the model (Marrelec, Kim, Doyon, & Horwitz, 2009; Salvador et al., 2005). This approach uses linear regression to remove temporal structure common to three or more brain regions, returning a measure of shared variance that is exclusive to each connection. The result is a network model that reflects connected regions in which unique information emerges, with connections that are conditionally independent, and thus can be defined as the effective connectivity of the network (Lee, Smyser, & Shimony, 2013; Smith et al., 2011; Marrelec et al., 2006, 2007). Because, however, connectivity models from partial correlations are undirected, we will refer to these partial correlation models as functional connectivity.

For our purposes, we have computed functional connectivity models from brain activity engaged in three key social tasks: face perception, action recognition, and the interpretation of interactivity from simple geometric shapes (Heider Simmel-like animations). Each of these tasks is associated with functional specialization in the pSTS and extended regions linked to the social perception and cognition (Saygin, Wilson, Hagler, Bates, & Sereno, 2004; Martin & Weisberg, 2003; Grossman & Blake, 2002; Hoffman & Haxby 2000). We used standard univariate approaches and a formal conjunction analysis to map brain regions common to all three localizers. We then computed an undirected, weighted network connectivity model using the partial correlation analysis. We further analyzed the network structure using metrics drawn from graph theory, a mathematical representation of a real-world complex system (e.g., large scale brain networks) defined by a collection of nodes (brain regions) and edges (anatomical, functional, or effective connections) connecting pairs of nodes (Minati, Varotto, D’Incerti, Panzica, & Chan, 2013; Bullmore & Sporns, 2009). Using these tools, we illustrate the unique connections between the pSTS and cortical regions that differentiate patterns of brain connectivity revealed by social perception localizers and characterize the functional specialization in their patterns of connectivity.

## **METHODS**

### **Participants**

A total of 16 individuals (8 men) from the University of California, Irvine, campus and community participated in this experiment. Participants completed two identical scanning sessions in two separate days. The Human Protections review board at the University of California, Irvine, approved all recruiting and consent procedures.

### **Localizers**

Volunteers participated in three localizer tasks (described below), all chosen because they identify brain regions associated with social perception and cognition (Figure 1).

#### *Biological Motion*

Point light animations depicting 25 unique actions were constructed using 13 black dots ( $0.17^\circ$  of visual angle) representing the major joints and head of an actor. The overall figure subtended approximately  $8^\circ \times 3.5^\circ$  of visual angle and was positioned at the center of the screen. Scrambled motion was constructed by randomizing the spatial location of the starting position dots while leaving the motion vectors intact. Blocks consisted of ten 1-sec animations with a 600-msec ISI. Participants performed a 1-back task (report a repeated animation) on each stimulus, with an average of three repeats within each block.

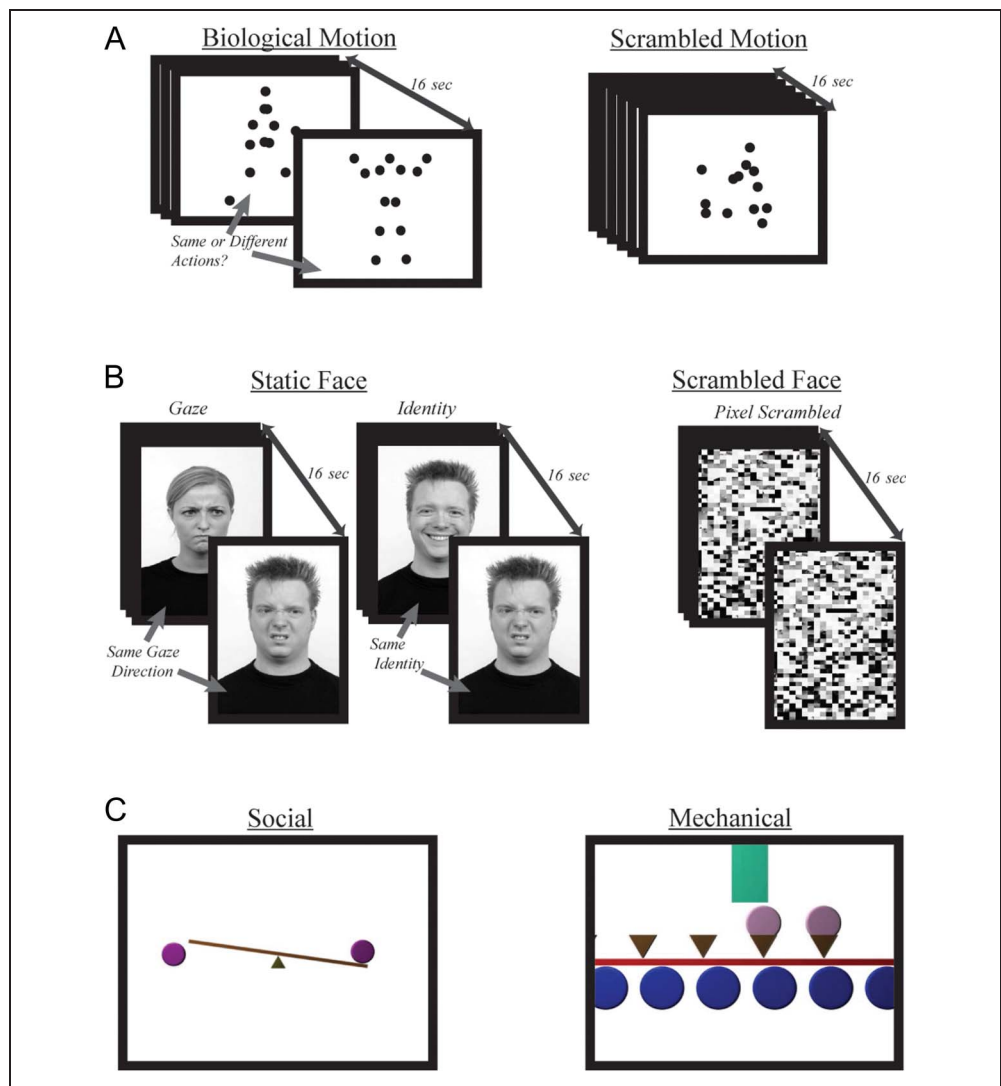
#### *Face Perception*

The face perception localizer was constructed similar to Haxby et al. (2001). Stationary grayscale images of faces ( $7.5^\circ \times 3^\circ$  visual angle) were obtained from the Radboud database (Langner et al., 2010), with all faces depicting adults in the frontal view with gaze directed to the left, right, or straight ahead and with happy, sad, angry, disgusted, or neutral emotional expression. Scrambled faces were created from the face images by pixel scrambling them in units of  $0.36^\circ$  visual angle. Each 16-sec block contained ten 750-msec images separated by 1000-msec ISI. During the face blocks, participants were cued to perform a 1-back task on the face identity (irrespective of facial expression or gaze direction) or gaze direction (irrespective of facial expression or identity) with five repeats per block (on average).

#### *Social Cognition*

The social cognition localizer was adapted from Martin and Weisberg (2003), with stimuli generously provided by Alex Martin. Participants viewed 21-sec video vignettes depicting geometric shapes moving such that they readily appeared as agents (self-motivated actors) engaged in

**Figure 1.** Schematic of stimuli used in the three core social cognitive localizers. (A) Point-light biological (left) and scrambled (right) motion. (B) Face and gaze recognition (left) and pixel scrambled images (right). (C) Vignettes of social interactions (left) and mechanical devices (right).



social interactions or as components of moving mechanical objects. Each vignette was immediately followed by a 6-sec response window with a multiple-choice selection in which participants selected one of four phrases that best described the preceding scene.

## Procedure

For both scanning sessions, biological motion and face perception localizers were implemented as blocked designs with six experimental blocks alternated with six control blocks, separated by 4-sec fixation intervals for a total of 12 blocks/scan. Blocks in the social cognition localizer extended to 27 sec and were separated by a 3-sec interblock interval, for a total of 8 blocks/scan. Each localizer scan was pseudorandomly presented twice within a single scanning session, for a total of 24 blocks/session for biological motion/face perception and 16 blocks/session for social cognition). All stimuli were displayed using

Psychophysics Toolbox (Brainard, 1997; Pelli, 1997) in MATLAB (The MathWorks, Inc., Natick, MA).

## Imaging

MR images were collected on the UCI 3T Philips Achieva scanner housed in the UCI Research Imaging Center and equipped with eight-channel parallel imaging. High-resolution anatomical images were acquired for each individual (T1-weighted MPRAGE, echo time = 3.7 msec, flip angle = 8°, 200 sagittal slices, 256 × 256 matrix, 1 × 1 × 1 mm<sup>3</sup> voxels). Functional images (single-shot, T2\*-weighted gradient EPI) were collected for the whole brain (2.0 × 2.0 × 4.0 mm<sup>3</sup>, echo time = 30 msec, flip angle = 90°, A-P phase encoding, 32 axial slices acquired interleaved, 0-mm gap between slices, SENSE factor = 2, repetition time = 2000 msec, 128 volumes). Participants viewed the animations through a periscope mirror mounted on the birdcage head-coil and directed

at a custom screen positioned at the head of the scanner. Responses were collected on an MR-compatible button box (Current Designs, Inc., Philadelphia, PA).

## Analysis

Functional images were corrected for motion within and across scans, coregistered to the individual participant's high-resolution anatomical images, and resampled into  $2 \times 2 \times 2$  mm voxels when transformed into standardized Talairach space (all conducted using BrainVoyager, Brain Innovation B.V., Maastricht, The Netherlands). Functional connectivity analyses were conducted in MATLAB.

### Whole-brain Conjunction Analysis

Localizers were analyzed using a group general linear model analysis with hemodynamic predictors estimating the blocked responses for the two conditions of interest (for each localizer scan). Significance for individual localizers was assessed at false discovery rate of  $q < 0.005$  (Genovese, Lazar, & Nichols, 2002). Following the formal conjunction analysis approach of Nichols, Brett, Andersson, Wager, and Poline (2005), conjunction voxels were identified as those with significantly higher activation in all of the three social cognitive localizer tasks (biological > scrambled motion, faces > scrambled faces, and social > mechanical vignettes). Voxels included in the conjunction analysis must have survived the false discovery significance threshold for all three independent localizers. This conjunction analysis revealed 1 unilateral and 11 bilateral ROIs (23 total) on which we conducted the functional connectivity analysis.

### Functional Connectivity Analysis

Functional connectivity was assessed as the strength of the partial correlation between all pairwise combinations of ROIs. All voxels within a given ROI were averaged and  $z$ -scored to create a single normalized time series for each brain region for each localizer and each participant. Connectivity was computed as the linear relationship between the time-locked time series from two ROIs after variance accounted for by other ROI time series has been removed. The partial correlation reflects the correlation between the residual variance, after the influences of other ROI time series have been removed (Marrelec et al., 2009). Group level network connectivity for each localizer was computed as the mean of the Fisher  $z$ -transformed individual subject correlation matrices.

The multiple correlation coefficient is an estimate of the combined influence of two or more variables on the observed variable. For our partial correlation connectivity analysis, a brain region's multiple correlation coefficient measures the amount of variance in the time series that can be explained by the influence of all the other nodes of the network.

Partial correlations matrices and multiple correlation scores were computed for all localizers for each participant. Significance was assessed with Monte Carlo simulations in which new ROI time series were constructed by randomly sampling (with replacement) from each original ROI time series to generate a new bootstrapped time series of the same length. The partial correlation matrices were computed for each iteration (out of a total of 5000 iterations), and the distributions of correlations expected by chance were thus constructed. This process was conducted for each participant, for each session, and for each localizer to assess significance thresholds for each connection. Partial correlation values that were two standard deviations from the mean of this distribution were determined to be significant.

## Graph Metrics

Graphical model statistics were computed via the Brain Connectivity Toolbox (Rubinov & Sporns, 2010). Graph density was computed as the proportion of significant connections out of the total possible number of connections for the entire graphical model, calculated separately for each participant and each localizer. Node density was computed on each of the brain regions as the proportion of significant connections out of the total possible connections, calculated separately for each task. Hubs were identified on the functional connectivity graph as those brain regions with node degree ranked in the top three for each task.

The pattern of connectivity for each hub was quantified across the three tasks using a metric of stability, which was computed as:

$$S_n = 1 - \left( \frac{\sum_{i=1}^{nodes} \bigcap_{j=1}^{tasks} c_{ij}}{\bigcup_{j=1}^{tasks} c_{ij}} \right)$$

where  $n$  is the node of interest and  $c$  is the binary connection weight (1 or 0) for the edge connecting nodes  $n$  and  $i$  in condition  $j$ . A stability index of 0 indicates no connections shared between the three tasks, whereas an index of 1 indicates the identical pattern of connections for all tasks. A low stability index is an indicator for functional specialization in the pattern of connectivity for that node, whereas a high stability index is indicative of general processing pathways across the domain of tasks tested.

Node symmetry for the hubs was quantified as

$$Y_n = \sum_{i=0}^{nodes} \frac{c_i \cap c'_i}{c_i \cup c'_i}$$

such that  $n$  is the ROI for which symmetry is computed, wherein  $c_i$  is the binary connection weight (1 or 0, thresholded for significance) in the group graph for the edge connecting node  $n$  and  $i$  in one hemisphere and  $c'_i$  indicates the connectivity weight for the edge connecting

the opposite hemisphere homologous edge connecting node  $c'$  and node  $i'$ . A symmetry score of 1 indicates identical connectivity patterns mirrored in the right and left homologous ROIs, whereas a score of 0 indicates no symmetry in the connectivity patterns. This metric is particularly helpful for identifying laterality bias in functional specialization as assessed from the pattern of connectivity arising from the targeted ROI.

To determine the impact of task on the strength of functional connectivity, we conducted a one-way repeated-measures ANOVA to compare the weighted partial correlation values of the right pSTS connections across the tasks. On the basis of the findings from the binary graphs, we computed paired samples  $t$  tests to make post hoc comparisons between the conditions for each connection.

## RESULTS

### Univariate Localization Analysis

The results from group univariate general linear model analysis of each localizer are shown in Figure 2, all thresholded at a false discovery rate of  $q < 0.005$  (Genovese et al., 2002). A comparison of the maps revealed both coactivated and unique patterns of activation for the three localizers. The biological motion, face, and social localizers all individually identified large regions of the pSTS, lateral occipitotemporal cortex (EBA/hMT+), fusiform gyrus, intraparietal sulcus (IPS), premotor cortex (PMC), IFG, and insula. These findings are very similar to previous reports using these localizer tasks (Grossman, Jardine, & Pyles, 2010; Saygin, 2007; Grill-Spector, Knouf, & Kanwisher,

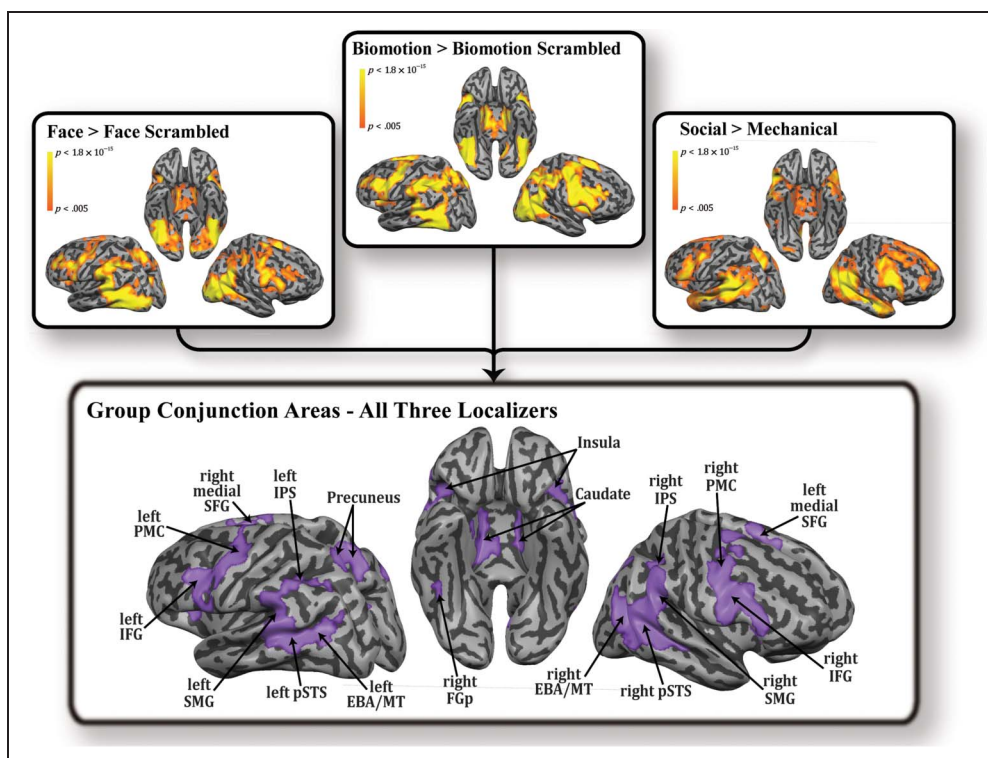
2004; Hoffman & Haxby, 2000). The social vignette localizer also identified large regions selective for social interactions extending the length of the STS (from the anterior pole to the most dorsal parietal aspects), IPS, and PMC.

Figure 2D shows the results of a formal conjunction applied to the three localizers, restricting the conjunction regions to those voxels that reached significance in all three tasks (Nichols et al., 2005; Figure 2 and Table 1). This map of conjunction areas identified large bilateral regions on the pSTS, lateral occipital cortex, fusiform gyrus, ventrolateral pFC, precuneus, and medial pFC. In total, the conjunction of the three localizers demarcated 1 unilateral and 11 bilateral regions (23 ROIs) coactivated by the localizers. These coactivated cortical regions served as the nodes for our functional connectivity analyses.

### Functional Connectivity Using Partial Correlation Analysis

Figure 3 shows the graphical representation of the group-averaged connectivity patterns computed from partial correlations between the ROIs identified in the conjunction of the three social cognitive localizer tasks. Each line on the graphical model indicates a connection between two brain regions in which significant, unique variance exists, after the influence of activity from all other brain regions has been removed (see Methods). Graphical models of connectivity computed using partial correlations are much less dense than task-based full correlation models because of the statistical removal of redundant variance in the connections. Our connectivity models

**Figure 2.** Group activation maps for each social perception localizer (top row) and the conjunction areas (bottom row). Top row maps define regions selectively activated by the experimental or control tasks, with significance assessed at a false discovery  $q < 0.005$ . Bottom row shows the group conjunction map of task-positive regions that were selectively activated in all conditions, as identified using a conjunction analysis.



**Table 1.** The Talairach Coordinates and the Volume of Regions of Interest Identified in the Formal Conjunction Analysis

		<i>Talairach Coordinates</i>			<i>ROI Size (mm<sup>3</sup>)</i>
		<i>ROI Centroid</i>			
	<i>ROI</i>	<i>x</i>	<i>y</i>	<i>z</i>	
Cerebellum	Left cerebellum	-18.4	-59.9	-31.0	27.6
	Right cerebellum	22.5	-55.4	-29.6	15.6
Temporal	Right fusiform	37.2	-43.3	-16.8	11.5
	Left EBA/MT	-44.0	-68.0	4.7	16.0
	Right EBA/MT	43.1	-62.7	3.5	25.0
	Left pSTS	-49.7	-47.2	5.7	16.9
	Right pSTS	47.4	-43.2	6.5	23.8
	Parietal	Left SMG	-49.8	-42.0	19.6
Right SMG		50.0	-37.6	25.7	8.4
Left IPS		-36.4	-50.8	32.8	19.4
Right IPS		37.1	-47.6	39.3	17.6
Medial	Left precuneus	-10.0	-65.2	42.1	20.6
	Right precuneus	0.9	-64.5	40.9	31.1
	Left caudate	-12.1	-4.0	13.9	25.5
	Right caudate	10.2	-7.6	12.6	28.5
Prefrontal	Left medial SFG	-5.8	7.9	49.7	6.8
	Right medial SFG	4.3	12.3	50.4	8.3
	Left PMC	-31.9	-8.3	51.1	25.5
	Right PMC	29.7	-5.1	50.8	26.0
	Left IFG	-38.7	9.2	28.6	22.1
	Right IFG	39.4	8.7	28.3	23.0
	Left insula	-36.3	17.4	8.87	17.3
	Right insula	36.1	17.6	9.03	15.6

SMG = supramarginal gyrus.

had an average connection density of 18.2%, which varied significantly across the three tasks ( $F(2, 30) = 4.67, p = .02$ ), with the fewest connections in the face localizer and the most in the social vignette localizer.

The graphical models shown in Figure 3 depict undirected, weighted edges between the respective nodes, with only connections that have a correlation strength greater than that expected by chance. Positive partial correlation coefficients (solid lines) indicate covariation in the residual variance of the two connected ROIs is time-locked and changing in the same direction (both increasing and decreasing for the specific condition/task). Similarly a negative correlation coefficient indicates antagonistic structure in the residual time series from the two connected ROIs (dashed lines in figure). Directionality of the correlation coefficient does not imply task-positive or task-negative activation (or deactivation). All

tasks revealed strong connectivity between homologous ROIs in the opposite hemispheres, as anticipated from previous literature (Salvador et al., 2005).

Graph metrics reveal important features in the pattern of connectivity emerging from the pSTS during these tasks. First, the right STS was consistently identified as the most highly connected or second most highly connected brain region among the 23 possible ROIs, regardless of task (Table 2, Connection Density). Together with the right PMC, the right pSTS was connected to an average of 30.4% of all possible ROIs in the network. It is important to point out that each of these connections reflects significant shared variance that is exclusive to the pSTS and connected node, unexplained by the temporal structure from any other node. Thus, the pSTS is an important network hub from which new, unique information emerges during the social perception tasks.

The bulk of these connections emerged between the pSTS and a set of core brain regions that were stable across the three localizers (Stability Index, Table 2). Core connections to the right pSTS include proximal connections (the right supramarginal gyrus and right EBA/hMT+), the homotopic connection (the left pSTS), and long-range connections to pFC (the right insula and right IFG). The pattern of connectivity derived from the group network maps was also apparent in the individual participants (Figure 4). Each of the connections between the pSTS and core regions in the group analysis was present (i.e., significantly stronger than anticipated by chance) in 75% or more of the individual participants. The findings reveal that the pSTS is a hub for neural communication that is not explained by the temporal variations in activation apparent in any other brain region included in our model.

As further evidence for a core social cognitive network, we found that the strengths of the core connections to the right pSTS had weights that did not vary as a function of task (Figure 5). We found no significant difference in the connectivity weights between the pSTS and any of the core regions when compared across the three localizers ( $F(2, 30) \leq 2.01$ , all  $ps \geq .15$ ).

The second most highly connected region in the network graph was the PMC. The PMC had connections both within and across hemispheres, most notably to the right EBA/hMT+ and right IPS in all localizers and bilaterally to the IPS in the biological motion perception localizer. This pattern of connections is characteristic of a subset of the mirror neuron network, most strongly engaged during action recognition. Perhaps even more interesting is that we found no evidence of connectivity between pSTS and PMC, either in the group connectivity maps or in individual participants. The implication is that any communication between these two regions reflects redundant information share variance with at least one other brain area in our network, not the emergence of new information structure.

Finally, the functional connectivity analysis, like univariate mapping studies, supports the model of right hemisphere dominance during the social perception localizers. The connections between pSTS and the core network were confined to right hemisphere ROIs (with the exception of the homotopic connection), with stronger connection weights overall from the right hemisphere pSTS as compared with homologous connections to the left hemisphere pSTS. Patterns of connectivity in the left pSTS during the face and social vignette localizers captured

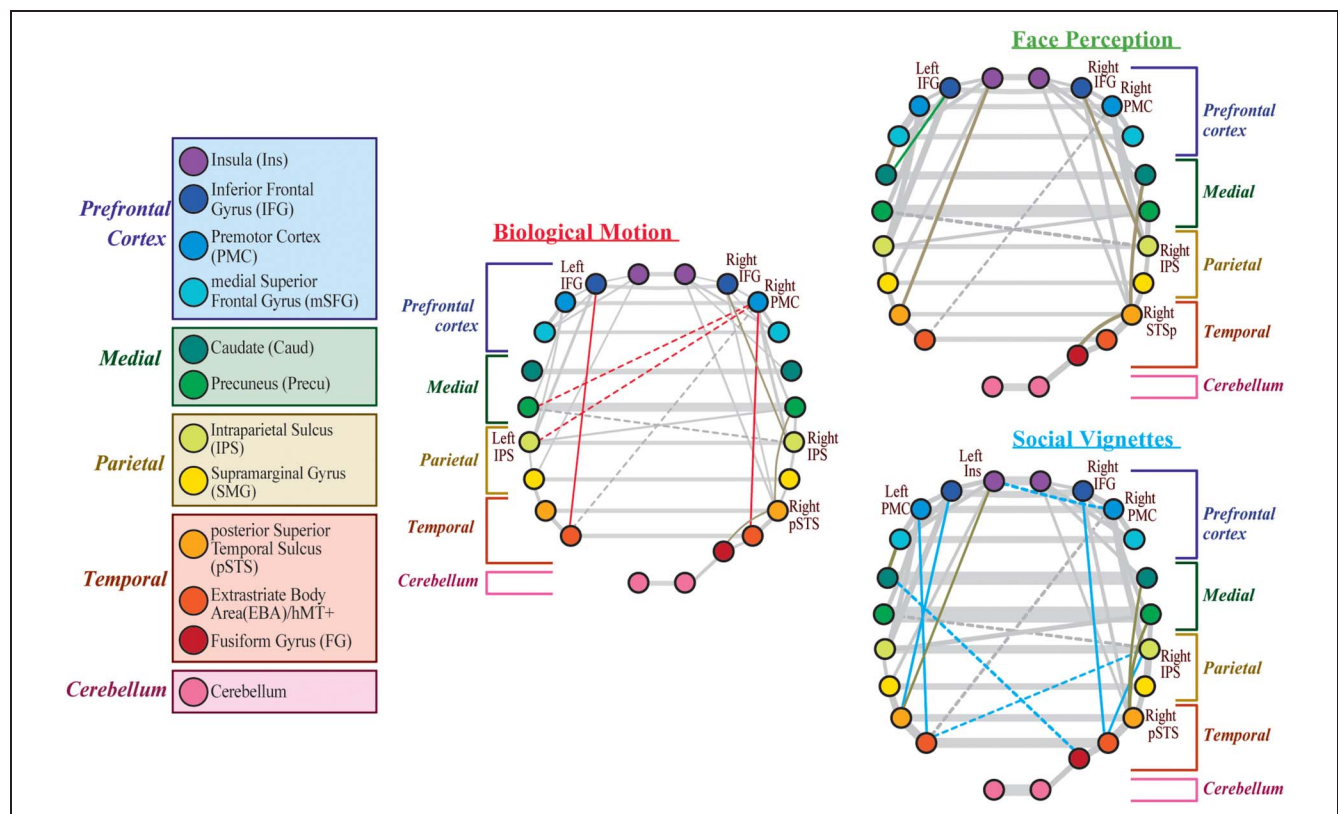


**Figure 3.** Network maps of effective connectivity for all ROIs (nodes) in the three localizer tasks. Lines (edges) denote shared unique variance among the two nodes, indicating significantly stronger connectivity than expected by chance. Connections common across two or more tasks are depicted in gray, whereas connections unique to a single task are color coded (red = biological motion; green = face perception; blue = social vignettes). Positive and negative significant partial correlations are depicted as solid and dashed lines, respectively, with the thickness of the line indicating the strength of connectivity.

**Table 2.** ROI Network Metrics

		<i>Node Density</i>				<i>Stability (%)</i>	<i>Symmetry (%)</i>			
							<i>0 = No Symmetry</i>			
	<i>ROI</i>	<i>Face</i>	<i>Bio</i>	<i>Social</i>	<i>Mean</i>		<i>Face</i>	<i>Bio</i>	<i>Social</i>	<i>Mean</i>
Cerebellum	Left cerebellum	4.3	4.3	4.3	4.30	19.6	19.8	19.8	33.5	24.37
	Right cerebellum	8.7	8.7	8.7	8.70	18.8				
Temporal	Right fusiform gyrus	13	13	13	13.00	19.8	–	–	–	–
	Left EBA/MT	17.4	13	21.7	17.37	21.4	39	39	42	40
	Right EBA/MT	17.4	13	21.7	17.37	26.2				
	Left pSTS	17.4	17.4	21.7	18.83	25.4	40.2	40.2	38.8	39.73
	Right pSTS	30.4	30.4	30.4	30.40	28.8				
Parietal	Left SPT	17.4	17.4	17.4	17.40	24.1	33.9	33.9	31.8	33.2
	Right SPT	13	13	13	13.00	21				
	Left IPS	26.1	21.7	21.7	23.17	26.3	34.3	34.3	41.2	36.6
	Right IPS	26.1	26.1	30.4	27.53	29.1				
Medial Wall	Left precuneus	21.7	17.4	17.4	18.83	27.6	32.8	31.9	27	30.57
	Right precuneus	26.1	21.7	26.1	24.63	25.2				
	Left caudate	4.3	13	13	10.10	23.8	28.5	27.3	29.7	28.5
	Right caudate	8.7	13	13	11.57	15.2				
Prefrontal	Left medial SFG	17.4	21.7	21.7	20.27	27.1	38.2	38.2	36.6	37.67
	Right medial SFG	17.4	17.4	17.4	17.40	26				
	Left PMC	21.7	21.7	26.1	23.17	32	44.8	44.8	41.6	43.73
	Right PMC	39.1	26.1	30.4	31.87	31.5				
	Left IFG	26.1	26.1	26.1	26.10	25.8	37.6	37.6	43.6	39.6
	Right IFG	26.1	26.1	26.1	26.10	28.7				
	Left insula	21.7	21.7	26.1	23.17	27.1	35.6	33.5	39.6	36.23
	Right insula	21.7	26.1	21.7	23.17	21.4				
	<i>Group means</i>	<i>17.4</i>	<i>18.1</i>	<i>19.2</i>	<i>18.2</i>	<i>25.1</i>	<i>35.0</i>	<i>34.6</i>	<i>36.9</i>	<i>35.5</i>

Graph metrics for the conjunction regions. Node density is the mean number of connections emerging from that node, computed separately for each individual. Instability quantifies the similarity of the connectivity pattern from each node across the three tasks. An instability score of 0 indicates unique connections for each task. A stability score of 100% indicates connections that are stable across all three tasks. Symmetry quantifies the number of connections that are mirrored in the right and left homologous regions (excluding the homotopic connection). A score of 0 indicates all unique connections, and 100% indicates complete symmetry. SPT = superior planum temporale.

fragments of the connections in the right hemisphere, but no new interregional connections (Table 2, Symmetry Index). In the strongest example of asymmetry, the left pSTS had no connectivity to pFC during the biological motion localizer. That the left hemisphere connectivity reveals no new patterns, only weaker ones, is evidence consistent with the proposal for right hemispheric dominance in social tasks.

The functional connectivity analysis also revealed a set of task-specific connections that include the right fusiform in the biological motion and face localizers, the caudate nucleus in the face and social vignette localizers, and the precuneus in the biological motion and social vignette localizers. Of

these task-sensitive connections, only the connection to fusiform gyrus was present in the majority of participants, and this was only during the biological motion and face localizers. This connection is consistent with recent findings of causal, directed connectivity between the pSTS and fusiform face area (FFA) during face and biological motion perception (Shultz, van den Honert, Engell, & McCarthy, 2015). Finally, those regions not connected in the group map were infrequently identified in individual participants.

We conclude that the key social localizers are very effective in identifying emergent information between a core, right hemisphere dominant network that connects pSTS to parietal cortex and pFC.

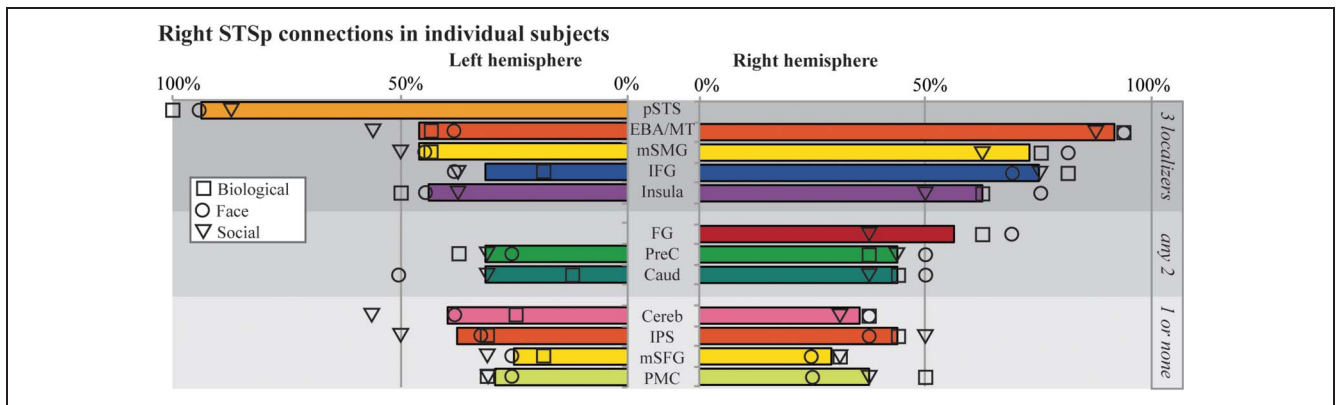


**Figure 4.** Percentage of individual participants in which connections to the right pSTS passed significance. Bar graphs reflect the group average across the three tasks with symbols identifying the individual task scores. ROIs are subdivided into the core connections (top group), connections present in the group analysis for at least one localizer (middle), and those regions that are not connected in any localizer (bottom). Bars are color coded to match the ROIs as shown in Figure 2 legend.

## DISCUSSION

The current study aims to understand information sharing within the network commonly identified in social cognitive localizer protocols. This approach is motivated by the premise that functional specialization of a given brain area includes its connectivity to other brain regions, a metric independent of the magnitude of selectivity derived from the univariate analyses of regional BOLD response. Using a formal conjunction analysis, we mapped 1 unilateral and 11 bilateral brain regions recruited in the perception and interpretation of social cognitive cues. All of these regions had univariate task-positive brain signals selective for the key localizers, and many have been identified as components of the social brain (Ishai, Schmidt, & Boesiger, 2005; Rotshtein, Henson, Treves, Driver, & Dolan, 2005; Ohnishi et al., 2004; Martin & Weisberg, 2003; Schultz et al., 2003; Beauchamp, Lee, Haxby, & Martin, 2002; Castelli, Frith, Happé, & Frith, 2002; Grossman & Blake, 2002; Vaina, Solomon, Chowdhury, Sinha, & Belliveau, 2001; Vuilleumier, Armony, Driver, & Dolan, 2001; Castelli, Happé, Frith, & Frith, 2000; Ishai,

Ungerleider, & Haxby, 2000; Kanwisher, McDermott, & Chun, 1997).

We analyzed functional connectivity among these regions using graphical modeling of the undirected partial correlations. Our analysis of the network configuration supports the hypothesis that the pSTS serves as a hub of the social brain network. The right pSTS was the most highly connected of the brain regions included in our model, with a core pattern of effectivity connectivity that was stable across the social localizers. The pSTS was strongly connected to regions associated with body and gaze perception (the EBA/hMT+ and IFG) but less strongly connected to the core regions of the mirror neuron network (PMC and the IPS). Unlike other highly connected regions, connectivity to the pSTS was distinctly lateralized, with more connections and more strongly weighted connections in the right hemisphere as compared with the left.

Because our approach was to identify those connections in which variance is exclusive to the two brain regions, we can conclude that this core social cognitive network reflects critical connections from which new neural information emerges when engaged in social cognitive tasks.

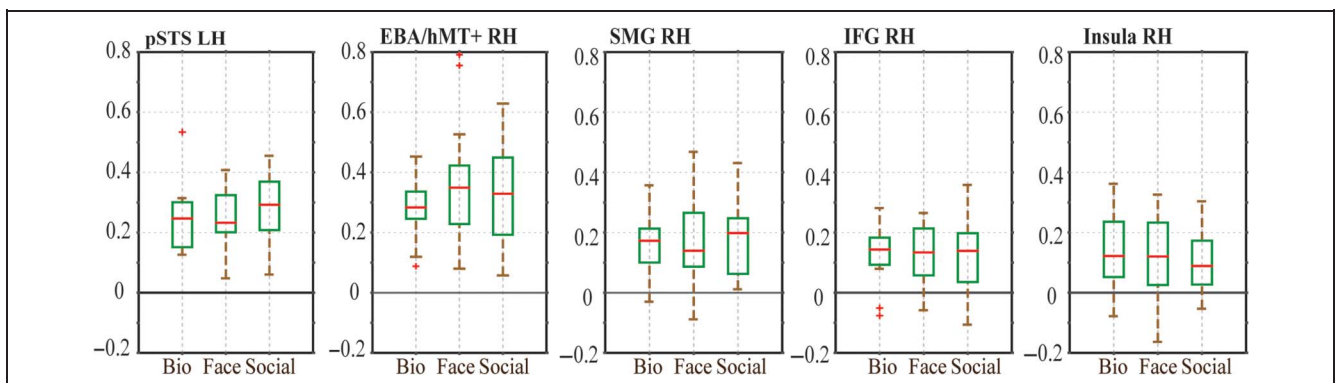


**Figure 5.** Individual participant weights for the core connections with the right pSTS during each localizer. Box median and whisker quartiles indicate individual participant variance among the 16 participants.

## The pSTS and the “Social Brain”

The notion that social perception and social cognition relies on large-scale brain networks has existed in the literature for over 20 years (Brothers, 1990). Defining the regions to be included in that network and the means of information sharing among them, however, has been significantly more complicated. In a recent analysis of the literature, Yang, Rosenblau, Keifer, and Pelphrey (2015) delineated three subnetworks that subservise discrete social cognitive tasks: perceptual and limbic regions that support perception of socially relevant cues, a frontoparietal “mirror neuron” network that supports the understanding and intent of actions, and a theory of mind network associated with the attribution of mental states to others. These networks are defined largely based on localization studies that map coactivated regions, with network structure implied by the higher frequency of coactivation among subsets of these regions. The pSTS is proposed as a potential hub across all the subnetworks, because it is the single brain region implicated in all three social domains. A similar finding was reported in a single experimental study (as opposed to a meta-analysis) using more naturalistic viewing of movies (Lahnakoski et al., 2012).

Our findings are the first to use large-scale network modeling to demonstrate hub and connectivity structure through models of partial correlation functional connectivity. These results are consistent with more targeted, smaller-scale dynamic causal modeling of effective connectivity between the pSTS and fusiform gyrus (Shultz et al., 2014). Those models indicate that the pSTS has causal influence on neural activity in the FFA during biological motion perception and the reverse directionality during face perception (with bidirectional connections for both). Thus, in both causal and large-scale undirected models, the pSTS is serving a critical role in social perceptual and cognitive tasks.

Interpreting the functional implications of these connections, however, can be quite complex. Action representations exist at multiple levels of abstraction, both within the pSTS and on the IFG. In a recent review, Lingnau and Downing (2015) argue for multiple topographies of action representation on the pSTS and the adjacent lateral occipital cortex, from feature-specific to abstract and inferential. Similarly, researchers propose multiple levels of action encoding in the IFG, from sensory-motor level (“concrete” encoding) to a more abstract semantic level (Kilner, 2011). Presumably some information as to how these events are encoded is apparent in the nature of the information communicated between these regions, but the specificity of that information is not yet clear.

We should note that our finding of strong connectivity between the pSTS and IFG is not without precedent. The IFG is implicated in face perception (van Kemenade, Muggleton, Walsh, & Saygin, 2012; Furl et al., 2010),

and a study of functional connectivity between core and extended face-responsive regions found the pSTS to be more strongly connected to the IFG than to regions in fusiform cortex during face perception (Davies-Thompson & Andrews, 2012). These pSTS to prefrontal connections are stronger specifically during tasks that require the interpretation of social cues (directed eye gaze) as compared with nonsocial cues (e.g., arrows; Callejas, Lupiáñez, & Tudela, 2004). Because our study isolated connections with unique variance (among all the variance considered within our model), our findings support the hypothesis that the information conveyed via this pathway is specialized in some way, which we hypothesize supports action observation. Our findings, therefore, go further than traditional mapping studies: Our functional connectivity implicates the pSTS as a hub for the emergence of new information within the social brain network.

## Relationship to PMC

We found a second hub of connectivity in PMC, which was also strongly modulated by the social perception localizers but not functionally connected to the pSTS. The pSTS and PMC are both implicated in the observation, understanding, and future imitation of actions, as demonstrated both through neuroimaging studies and through lesion analysis (Saygin, 2007; Saygin et al., 2004; Wheaton, Thompson, Syngeniotis, Abbott, & Puce, 2004). Neurons in the pSTS and PMC form an important core of the proposed mirror neuron network, linked to both the observation and execution of actions (Caggiano et al., 2011; Kilner, 2011; Nelissen et al., 2011; Carey, Perrett, & Oram, 1997; Gallese, Fadiga, Fogassi, & Rizzolatti, 1996). Although connectivity was not explicitly tested in the previous studies, the pSTS has been widely implicated as providing essential analysis of visual cues that are required for action understanding and is generally considered a core input region to the larger action observation network. And yet we find that the two regions do not share a unique variance and thus are not the source of new, emergent neural processing.

This raises the question as to how to interpret the relationship between brain areas that are modulated by the task in the univariate response, but not functionally connected. Network structure can be computed using a number of different approaches, each of which has strengths and limitations in the extent to which they can reveal the underlying network structure. Connectivity as computed through partial correlations is among the most sensitive measures for detecting network structure embedded within distributed sources of nuisance variance (Smith et al., 2011).

The strength of this approach is that the partial correlations isolate variance in the neural signal uniquely shared between two nodes, with the redundant and distributed sources of variance removed (Sun, Miller, &

D'Esposito, 2004). There are many fewer connections in this type of model as compared with a full correlation model (approximately 20% of all possible connections), with the implication that each of these edges is more likely to reflect functionally relevant patterns of information sharing that those identified using more traditional approaches. Because all the regions included in our model were positively modulated by the three social cognitive localizers, each is presumed to have information relevant to the tasks. The functional connectivity model, however, reduces those connections down to only those with temporal variations in the time series exclusive to the two ROIs. Thus, it is not surprising that brain areas with univariate responses modulated during the same conditions may not be connected in the model. Brain regions A and B that are both modulated by a given task but not connected in the functional connectivity model share variance with a third brain region C. Although some investigators would label edges between A, B, and C as spurious, we interpret these connections as “redundant” because the information is distributed (Marrelec et al., 2006).

Determining the source of the underlying driving variable would be helpful in interpreting each of these circumstances, but in practice that is quite difficult. For example, subject motion artificially inflates functional connectivity estimates from traditional Pearson's  $r$  correlations, creating spurious correlations not reflecting intrinsic connectivity (Power et al., 2012). Partial correlation is a good approach to remove that nuisance variance (Satterthwaite et al., 2012).

A final consideration is the likelihood that ROIs identified with robust localizers (such as the ones used in our study) likely include regional activations that reflect the sum of multiple sources originating from subregions within. For example, the pSTS may have subregions more selective for discriminating eye gaze over identity, but these would not be discernable in our statistical contrast of faces with scrambled images of faces. Multivariate pattern decomposition approaches, such as independent component analysis, may be effective for isolating subregions from within these relatively large ROIs but would do so at the loss of information derived from the temporal patterns that we have analyzed here. Further work will determine whether refinements on these localizers, which would no doubt limit the ROIs selection, would introduce refinements on our model.

### **Right Hemisphere Specialization**

Previous fMRI mapping studies identify asymmetries in the organization of functional maps supporting social cognitive tasks, including action recognition (Saxe, Xiao, Kovacs, Perrett, & Kanwisher, 2004), social decision-making, and emotional processing. Studies done on functional specialization of pSTS commonly find hemispheric asymmetries with a right pSTS dominance (right identified more frequently and with stronger levels of activation than the left) for human face perception, move-

ment perception, and understanding (Herrington, Nymberg, & Schultz, 2011; Vander Wyk, Hudac, Carter, Sobel, & Pelphrey, 2009; Thompson, Hardee, Panayiotou, Crewther, & Puce, 2007; Pelphrey, Morris, & McCarthy, 2004; Pelphrey, Viola & McCarthy, 2004). With regard to brain connectivity, patients with right-lateralized lesions in ventromedial pFC tend to have more severe deficits in social decision-making and emotional processing tasks (Tranel, Bechara, & Denburg, 2002). Laterality, therefore, is a defining feature of the social cognitive brain systems.

In our measurement of functional connectivity, we found a clear asymmetry in the number and strength of connections between the right and left pSTS. The right pSTS had more connections (predominantly long range to pFC) than the left pSTS, apparent in the group network map and in the number of individual participants in which connections surpassed critical significance thresholds. When symmetry was tested explicitly, the patterns of connectivity emerging from the right pSTS were only partially apparent in the left, with no new interregional connections in the left pSTS. These metrics implicate the right, but not left, pSTS as a critical information-sharing hub that is sensitive to the unique demands of face recognition, action recognition, and social cognitive vignette tasks.

### **Relationship to the “Causal” Literature**

A final consideration is the link between network models of social perception networks and theories of functional specialization drawn from cortical anomalies. There is very little indication that generalized social cognitive deficits result from acute and localized insult to the pSTS, although there is at least one case of an individual that failed to properly ascertain eye gaze as a consequence of a stroke impacting the right STS (Akiyama et al., 2006). Right parietal stroke patients have difficulty perceiving biological motion from point-light sequences, although these deficits are linked to attentionally guided cognitive mechanisms more generally, not the perception of social cues per se (Battelli et al., 2001).

The strongest model of social cognitive dysfunction is autism, which is associated with atypical patterns of long-range functional connectivity as compared with neurotypicals in the social cognition brain network (specifically hypoconnectivity, Hadjikhani, Joseph, Snyder, & Tager-Flusberg, 2007; also as assessed in the resting state; von dem Hagen et al., 2013; Anderson et al., 2011). The pSTS as a hub is reduced in autism spectrum disorder as compared with the typical brain and regional hypoconnectivity throughout the networks identified in our study (Itahashi et al., 2014; Kana, Libero, Hu, Deshpande, & Colburn, 2014; Uddin & Menon, 2009; Koshino et al., 2008). Long-range connectivity patterns including interhemispheric connections are also decreased in autism spectrum disorder patients. Together these findings in the neuropsychological literature indicate that social perception is not well characterized by a localizationist approach.

## Conclusions

There has been much previous work linking the human pSTS (and the likely monkey homologue, the anterior STS) to visual analysis of social cues (Puce & Perrett, 2003). Indeed, the response of individual neurons to a given action and the pattern of activity measured across the STS depend not just on the nature of the external social cues but also on context and how the observer interprets them (Vander Wyk, Voos, & Pelphrey, 2012; Pelphrey & Morris, 2006). For example, large-scale brain networks identified during social cognitive tasks can be separated into subnetworks specialized for identifying agency (“who”), recognizing actions (“what”), or making inferences about goals and mental states of others (“why”; Spreng, Stevens, Chamberlain, Gilmore, & Schacter, 2010; Van Overwalle, 2009). Thus we argue that the functional importance of pSTS cannot be studied in an isolated manner, without considering its role in the large-scale network of brain regions involved in various aspects of social cognition.

## Acknowledgments

This material is based on work supported by the National Science Foundation under NSF BCS0748314 awarded to E. Grossman.

Reprint requests should be sent to Emily D. Grossman, Department of Cognitive Sciences, University of California, Irvine, 3151 Social Science Plaza, Irvine, CA 92697-5100, or via e-mail: grossman@uci.edu.

## REFERENCES

- Akiyama, T., Kato, M., Muramatsu, T., Saito, F., Umeda, S., & Kashima, H. (2006). Gaze but not arrows: A dissociative impairment after right superior temporal gyrus damage. *Neuropsychologia*, *44*, 1804–1810.
- Anderson, J. S., Nielsen, J. A., Froehlich, A. L., DuBray, M. B., Druzgal, T. J., Cariello, A. N., et al. (2011). Functional connectivity magnetic resonance imaging classification of autism. *Brain*, *134*, 3742–3754.
- Battelli, L., Cavanagh, P., Intriligator, J., Tramo, M. J., Hénaff, M. A., Michèl, F., et al. (2001). Unilateral right parietal damage leads to bilateral deficit for high-level motion. *Neuron*, *32*, 985–995.
- Beauchamp, M. S., Lee, K. E., Haxby, J. V., & Martin, A. (2002). Parallel visual motion processing streams for manipulable objects and human movements. *Neuron*, *34*, 149–159.
- Brainard, D. H. (1997). The Psychophysics Toolbox. *Spatial Vision*, *10*, 433–436.
- Brothers, L. (1990). The neural basis of primate social communication. *Motivation and Emotion*, *14*, 81–91.
- Bullmore, E., & Sporns, O. (2009). Complex brain networks: Graph theoretical analysis of structural and functional systems. *Nature Reviews Neuroscience*, *10*, 186–198.
- Caggiano, V., Fogassi, L., Rizzolatti, G., Pomper, J. K., Thier, P., Giese, M. A., et al. (2011). View-based encoding of actions in mirror neurons of area F5 in macaque premotor cortex. *Current Biology*, *21*, 144–148.
- Callejas, A., Lupiáñez, J., & Tudela, P. (2004). The three attentional networks: On their independence and interactions. *Brain and Cognition*, *54*, 225–227.
- Carey, D. P., Perrett, D. I., & Oram, M. W. (1997). Recognizing, understanding and reproducing action. *Handbook of Neuropsychology*, *11*, 111–130.
- Carrington, S. J., & Bailey, A. J. (2009). Are there theory of mind regions in the brain? A review of the neuroimaging literature. *Human Brain Mapping*, *30*, 2313–2335.
- Carter, R. M., & Huettel, S. A. (2013). A nexus model of the temporal–parietal junction. *Trends in Cognitive Sciences*, *17*, 328–336.
- Caspers, S., Zilles, K., Laird, A. R., & Eickhoff, S. B. (2010). ALE meta-analysis of action observation and imitation in the human brain. *Neuroimage*, *50*, 1148–1167.
- Castelli, F., Frith, C., Happé, F., & Frith, U. (2002). Autism, Asperger syndrome and brain mechanisms for the attribution of mental states to animated shapes. *Brain*, *125*, 1839–1849.
- Castelli, F., Happé, F., Frith, U., & Frith, C. (2000). Movement and mind: A functional imaging study of perception and interpretation of complex intentional movement patterns. *Neuroimage*, *12*, 314–325.
- Davies-Thompson, J., & Andrews, T. J. (2012). Intra- and interhemispheric connectivity between face-selective regions in the human brain. *Journal of Neurophysiology*, *108*, 3087–3095.
- Furl, N., van Rijsbergen, N. J., Kiebel, S. J., Friston, K. J., Treves, A., & Dolan, R. J. (2010). Modulation of perception and brain activity by predictable trajectories of facial expressions. *Cerebral Cortex*, *20*, 694–703.
- Gallese, V., Fadiga, L., Fogassi, L., & Rizzolatti, G. (1996). Action recognition in the premotor cortex. *Brain*, *119*, 593–610.
- Genovese, C. R., Lazar, N. A., & Nichols, T. (2002). Thresholding of statistical maps in functional neuroimaging using the false discovery rate. *Neuroimage*, *15*, 870–878.
- Gobbini, M. I., Koralek, A. C., Bryan, R. E., Montgomery, K. J., & Haxby, J. V. (2007). Two takes on the social brain: A comparison of theory of mind tasks. *Journal of Cognitive Neuroscience*, *19*, 1803–1814.
- Grill-Spector, K., Knouf, N., & Kanwisher, N. (2004). The fusiform face area subserves face perception, not generic within-category identification. *Nature Neuroscience*, *7*, 555–562.
- Grossman, E. D., & Blake, R. (2002). Brain areas active during visual perception of biological motion. *Neuron*, *35*, 1167–1175.
- Grossman, E. D., Jardine, N. L., & Pyles, J. A. (2010). fMR-adaptation reveals invariant coding of biological motion on the human STS. *Frontiers in Human Neuroscience*, *4*, 1–18.
- Hadjikhani, N., Joseph, R. M., Snyder, J., & Tager-Flusberg, H. (2007). Abnormal activation of the social brain during face perception in autism. *Human Brain Mapping*, *28*, 441–449.
- Hein, G., & Knight, R. T. (2008). Superior temporal sulcus—It’s my area: Or is it?. *Journal of Cognitive Neuroscience*, *20*, 2125–2136.
- Herrington, J. D., Nymberg, C., & Schultz, R. T. (2011). Biological motion task performance predicts superior temporal sulcus activity. *Brain and Cognition*, *77*, 372–381.
- Hoffman, E. A., & Haxby, J. V. (2000). Distinct representations of eye gaze and identity in the distributed human neural system for face perception. *Nature Neuroscience*, *3*, 80–84.
- Ishai, A., Schmidt, C. F., & Boesiger, P. (2005). Face perception is mediated by a distributed cortical network. *Brain Research Bulletin*, *67*, 87–93.
- Ishai, A., Ungerleider, L. G., & Haxby, J. V. (2000). Distributed neural systems for the generation of visual images. *Neuron*, *28*, 979–990.

- Itahashi, T., Yamada, T., Watanabe, H., Nakamura, M., Jimbo, D., Shioda, S., et al. (2014). Altered network topologies and hub organization in adults with autism: A resting-state fMRI study. *PLoS One*, *9*, e94115.
- Kana, R. K., Libero, L. E., Hu, C. P., Deshpande, H. D., & Colburn, J. S. (2014). Functional brain networks and white matter underlying theory-of-mind in autism. *Social Cognitive and Affective Neuroscience*, *9*, 98–105.
- Kanwisher, N., McDermott, J., & Chun, M. M. (1997). The fusiform face area: A module in human extrastriate cortex specialized for face perception. *Journal of Neuroscience*, *17*, 4302–4311.
- Kilner, J. M. (2011). More than one pathway to action understanding. *Trends in Cognitive Sciences*, *15*, 352–357.
- Koshino, H., Kana, R. K., Keller, T. A., Cherkassky, V. L., Minshew, N. J., & Just, M. A. (2008). fMRI investigation of working memory for faces in autism: Visual coding and underconnectivity with frontal areas. *Cerebral Cortex*, *18*, 289–300.
- Krueger, F., Barbey, A. K., & Grafman, J. (2009). The medial prefrontal cortex mediates social event knowledge. *Trends in Cognitive Sciences*, *13*, 103–109.
- Lahnakoski, J. M., Glerean, E., Salmi, J., Jääskeläinen, I. P., Sams, M., Hari, R., et al. (2012). Naturalistic fMRI mapping reveals superior temporal sulcus as the hub for the distributed brain network for social perception. *Frontiers in Human Neuroscience*, *6*, 1–14.
- Langner, O., Dotsch, R., Bijlstra, G., Wigboldus, D. H. J., Hawk, S. T., & van Knippenberg, A. (2010). Presentation and validation of the Radboud Faces Database. *Cognition & Emotion*, *24*, 1377–1388.
- Lee, M. H., Smyser, C. D., & Shimony, J. S. (2013). Resting-state fMRI: A review of methods and clinical applications. *American Journal of Neuroradiology*, *34*, 1866–1872.
- Lingnau, A., & Downing, P. E. (2015). The lateral occipitotemporal cortex in action. *Trends in Cognitive Sciences*, *19*, 268–277.
- Marrelec, G., Horwitz, B., Kim, J., Pélégrini-Issac, M., Benali, H., & Doyon, J. (2007). Using partial correlation to enhance structural equation modeling of functional MRI data. *Magnetic Resonance Imaging*, *25*, 1181–1189.
- Marrelec, G., Kim, J., Doyon, J., & Horwitz, B. (2009). Large scale neural model validation of partial correlation analysis for effective connectivity investigation in functional MRI. *Human Brain Mapping*, *30*, 941–950.
- Marrelec, G., Krainik, A., Duffau, H., Pélégrini-Issac, M., Lehericy, S., Doyon, J., et al. (2006). Partial correlation for functional brain interactivity investigation in functional MRI. *Neuroimage*, *32*, 228–237.
- Martin, A., & Weisberg, J. (2003). Neural foundations for understanding social and mechanical concepts. *Cognitive Neuropsychology*, *20*, 575–587.
- Menon, V., & Uddin, L. Q. (2010). Saliency, switching, attention and control: A network model of insula function. *Brain Structure and Function*, *214*, 655–667.
- Miller, E. K., & Cohen, J. D. (2001). An integrative theory of prefrontal cortex function. *Annual Review of Neuroscience*, *24*, 167–202.
- Minati, L., Varotto, G., D’Incerti, L., Panzica, F., & Chan, D. (2013). From brain topography to brain topology: Relevance of graph theory to functional neuroscience. *NeuroReport*, *24*, 536–543.
- Nelissen, K., Borra, E., Gerbella, M., Rozzi, S., Luppino, G., Vanduffel, W., et al. (2011). Action observation circuits in the macaque monkey cortex. *Journal of Neuroscience*, *31*, 3743–3756.
- Nichols, T., Brett, M., Andersson, J., Wager, T., & Poline, J. B. (2005). Valid conjunction inference with the minimum statistic. *Neuroimage*, *25*, 653–660.
- Ohnishi, T., Moriguchi, Y., Matsuda, H., Mori, T., Hirakata, M., Imabayashi, E., et al. (2004). The neural network for the mirror system and mentalizing in normally developed children: An fMRI study. *NeuroReport*, *15*, 1483–1487.
- Pelli, D. G. (1997). The Video Toolbox software for visual psychophysics: Transforming numbers into movies. *Spatial Vision*, *10*, 437–442.
- Pelphrey, K. A., & Morris, J. P. (2006). Brain mechanisms for interpreting the actions of others from biological-motion cues. *Current Directions in Psychological Science*, *15*, 136–140.
- Pelphrey, K. A., Morris, J. P., & McCarthy, G. (2004). Grasping the intentions of others: The perceived intentionality of an action influences activity in the superior temporal sulcus during social perception. *Journal of Cognitive Neuroscience*, *16*, 1706–1716.
- Pelphrey, K. A., Viola, R. J., & McCarthy, G. (2004). When strangers pass processing of mutual and averted social gaze in the superior temporal sulcus. *Psychological Science*, *15*, 598–603.
- Power, J. D., Barnes, K. A., Snyder, A. Z., Schlaggar, B. L., & Petersen, S. E. (2012). Spurious but systematic correlations in functional connectivity MRI networks arise from subject motion. *Neuroimage*, *59*, 2142–2154.
- Puce, A., & Perrett, D. (2003). Electrophysiology and brain imaging of biological motion. *Philosophical Transactions of the Royal Society of London, Series B, Biological Sciences*, *358*, 435–445.
- Rotshtein, P., Henson, R. N., Treves, A., Driver, J., & Dolan, R. J. (2005). Morphing Marilyn into Maggie dissociates physical and identity face representations in the brain. *Nature Neuroscience*, *8*, 107–113.
- Rubinov, M., & Sporns, O. (2010). Complex network measures of brain connectivity: Uses and interpretations. *Neuroimage*, *52*, 1059–1069.
- Salvador, R., Suckling, J., Coleman, M. R., Pickard, J. D., Menon, D., & Bullmore, E. D. (2005). Neurophysiological architecture of functional magnetic resonance images of human brain. *Cerebral Cortex*, *15*, 1332–1342.
- Satterthwaite, T. D., Wolf, D. H., Loughhead, J., Ruparel, K., Elliot, M. A., Hakonarson, H., et al. (2012). Impact of in-scanner head motion on multiple measures of functional connectivity: Relevance for studies of neurodevelopment in youth. *Neuroimage*, *60*, 623–632.
- Saxe, R., Xiao, D. K., Kovacs, G., Perrett, D. I., & Kanwisher, N. (2004). A region of right posterior superior temporal sulcus responds to observed intentional actions. *Neuropsychologia*, *42*, 1435–1446.
- Saygin, A. P. (2007). Superior temporal and premotor brain areas necessary for biological motion perception. *Brain: A Journal of Neurology*, *130*, 2452–2461.
- Saygin, A. P., Wilson, S. M., Hagler, D. J., Bates, E., & Sereno, M. I. (2004). Point-light biological motion perception activates human premotor cortex. *Journal of Neuroscience*, *24*, 6181–6188.
- Schultz, R. T., Grelotti, D. J., Klin, A., Kleinman, J., Van der Gaag, C., Marois, R., et al. (2003). The role of the fusiform face area in social cognition: Implications for the pathobiology of autism. *Philosophical Transactions of the Royal Society of London, Series B, Biological Sciences*, *358*, 415–427.
- Shultz, S., & McCarthy, G. (2012). Goal-directed actions activate the face-sensitive posterior superior temporal sulcus and fusiform gyrus in the absence of human-like perceptual cues. *Cerebral Cortex*, *22*, 1098–1106.
- Shultz, S., van den Honert, R. N., Engell, A. D., & McCarthy, G. (2015). Stimulus-induced reversal of information flow through a cortical network for animacy perception. *Social Cognitive and Affective Neuroscience*, *19*, 129–135.

- Smith, S. M., Miller, K. L., Salimi-Khorshidi, G., Webster, M., Beckmann, C. F., Nichols, T. E., et al. (2011). Network modelling methods for fMRI. *Neuroimage*, *54*, 875–891.
- Spreng, R. N., Stevens, W. D., Chamberlain, J. P., Gilmore, A. W., & Schacter, D. L. (2010). Default network activity, coupled with the frontoparietal control network, supports goal-directed cognition. *Neuroimage*, *53*, 303–317.
- Sun, F. T., Miller, L. M., & D'Esposito, M. (2004). Measuring interregional functional connectivity using coherence and partial coherence analyses of fMRI data. *Neuroimage*, *21*, 647–658.
- Thompson, J. C., Hardee, J. E., Panayiotou, A., Crewther, D., & Puce, A. (2007). Common and distinct brain activation to viewing dynamic sequences of face and hand movements. *Neuroimage*, *37*, 966–973.
- Tranel, D., Bechara, A., & Denburg, N. L. (2002). Asymmetric functional roles of right and left ventromedial prefrontal cortices in social conduct, decision-making, and emotional processing. *Cortex*, *38*, 589–612.
- Uddin, L. Q., & Menon, V. (2009). The anterior insula in autism: Under-connected and under-examined. *Neuroscience & Biobehavioral Reviews*, *33*, 1198–1203.
- Vaina, L. M., Solomon, J., Chowdhury, S., Sinha, P., & Belliveau, J. W. (2001). Functional neuroanatomy of biological motion perception in humans. *Proceedings of the National Academy of Sciences, U.S.A.*, *98*, 11656–11661.
- van Kemenade, B. M., Muggleton, N., Walsh, V., & Saygin, A. P. (2012). Effects of TMS over premotor and superior temporal cortices on biological motion perception. *Journal of Cognitive Neuroscience*, *24*, 896–904.
- Van Overwalle, F. (2009). Social cognition and the brain: A meta-analysis. *Human Brain Mapping*, *30*, 829–858.
- Vander Wyk, B. C., Hudac, C. M., Carter, E. J., Sobel, D. M., & Pelphrey, K. A. (2009). Action understanding in the superior temporal sulcus region. *Psychological Science*, *20*, 771–777.
- Vander Wyk, B. C., Voos, A., & Pelphrey, K. A. (2012). Action representation in the superior temporal sulcus in children and adults: An fMRI study. *Developmental Cognitive Neuroscience*, *2*, 409–416.
- von dem Hagen, E. A., Stoyanova, R. S., Rowe, J. B., Baron-Cohen, S., & Calder, A. J. (2013). Direct gaze elicits atypical activation of the theory-of-mind network in autism spectrum conditions. *Cerebral Cortex*, bht003.
- Vuilleumier, P., Armony, J. L., Driver, J., & Dolan, R. J. (2001). Effects of attention and emotion on face processing in the human brain: An event-related fMRI study. *Neuron*, *30*, 829–841.
- Wheaton, K. J., Thompson, J. C., Syngieniotis, A., Abbott, D. F., & Puce, A. (2004). Viewing the motion of human body parts activates different regions of premotor, temporal, and parietal cortex. *Neuroimage*, *22*, 277–288.
- Yang, D. Y. J., Rosenblau, G., Keifer, C., & Pelphrey, K. A. (2015). An integrative neural model of social perception, action observation, and theory of mind. *Neuroscience & Biobehavioral Reviews*, *51*, 263–275.